PHYSICAL REVIEW A VOLUME 27, NUMBER 4 APRIL 1983

Photoexcitation of an autoionizing resonance in the presence of off-diagonal relaxation

K. Rzążewski* and J. H. Eberly
Department of Physics and Astronomy, University of Rochester, Rochester, New York 14627
(Received 30 July 1982)

We discuss the theory of photoexcitation of an autoionizing resonance. We solve a set of coupled stochastic integrodifferential equations which are based on the Fano model for autoionization, but which include the effects of weak elastic collisions, weak or strong laser excitation, and finite laser bandwidth. We determine the exact photoelectron spectrum and give formulas for spectral peak positions and widths. Redistributive scattering is evident, as are various effects normally associated only with transitions between discrete levels. Under certain conditions symmetries and fixed points of the electron spectrum can be predicted.

I. INTRODUCTION

Certain phenomena that are common in bound-bound radiative transitions are typically not observed at all in bound-free transitions. For example, stimulated emission is not normally considered to be a process that accompanies photoionization. In this paper we discuss atypical situations, in which bound-free transitions may exhibit effects that are unusually similar to those found in bound-bound transitions, without requiring unusually powerful laser excitation. All of these effects are associated with repeated coherent continuum-to-bound electronic recombination.

We have made a nonperturbative theoretical study of bound-to-continuum radiative transitions in which the continuum electron state is an autoionizing state which is reached by near-resonant laser excitation from a lower discrete state. We have extended the Fano atomic model[1] of autoionization (see Fig. 1) and have included effects of "transverse" or off-diagonal relaxation. In this paper we concentrate on the details of the photoelectron spectrum, and describe the results of the interference of the transition between discrete states $|0\rangle$ and $|1\rangle$ with the transition between $|0\rangle$ and the continuum. Balance between the coupling strengths associated with these transitions defines a threshold for the onset of significant changes in the photoelectron line shape. In some situations this threshold is rather low, and it can be altered significantly by off-diagonal relaxation.

We have already discussed, in a paper[2] we will designate as RE for convenience, the existence and location of a certain "confluence" of laser-atom coherences, when the exciting laser power is a few times greater than the threshold just mentioned. An earlier paper of Lambropoulos[3] contained numerical evidence for such a confluence in free-free transitions, and Lambropoulos and Zoller[3] have analyzed the bound-free case using a model slightly different from ours. Subsequently, Agarwal *et al.*[4] have enlarged the scope of these studies by including some effects of radiative relaxation (i.e., spontaneous emission) without giving up the nonperturbative character of the earlier work. Other theoretical studies that also deal with aspects of laser-induced coherences in autoionization have been presented by Armstrong *et al.*,[5] Heller *et al.*,[6] Coleman and Knight,[7] and Andryushin *et al.*[8]

In the present paper we will explain the details of the calculations presented in RE, and expand the scope of these studies further by considering the effect of phase relaxation on the transitions. Such transverse or off-diagonal relaxation affects the relative phase between the atomic dipole moment and the electric field of the incident laser. It may be due, for example, to soft elastic collisions of the atoms, or to laser phase fluctuations. As we show, the effects of phase relaxation can be different from the effects discussed by Agarwal *et al.* The differences arise because radiative relaxation is a type of lifetime relaxation, associated with a fixed ratio between diagonal and off-diagonal relaxation rates: $\gamma_d/\gamma_{od}=2$, whereas phase diffusion contributes only off-diagonal relaxation. The greatest physical difference between these complementary relaxation models is that purely off-diagonal relaxation permits redistributive scattering,[9] whereas radiative relaxation (along with other lifetime relaxation mechanisms) does not.

In Sec. II we discuss the model that we use for the atom. It is a two-Lorentzian generalization of Fano's model, and is characterized by the same asymmetry parameter of Fano, denoted q. In Sec. III we introduce our relaxation model and identify

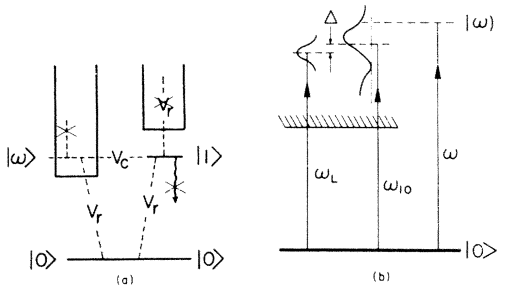

FIG. 1. (a) Schematic electron energy levels showing degeneracy of discrete level $|1\rangle$ and a continuum level $|\omega\rangle$. The (Coulombic) interaction V_c mixes $|1\rangle$ and $|\omega\rangle$. Both $|1\rangle$ and $|\omega\rangle$ are connected to $|0\rangle$ via the radiative interaction V_r. Crosses show that a number of possible interactions (radiative decay, continuum-continuum transitions, etc.) are artificially supressed in the model. (b) Schematic energy levels of the same atom after the Hamiltonian is partially rediagonalized to account for the Coulombic mixing, following Fano (Ref. 1). Only continuum states $|\omega\rangle$, superpositions of $|1\rangle$ and $|\omega\rangle$, remain above the ionization threshold. The original $|1\rangle$-$|0\rangle$ transition frequency ω_{10} is related to the laser frequency ω_L by the offset Δ (the detuning). Spread of frequencies at the end of the ω_L arrow indicates an uncertainty due to laser bandwidth or collisions.

the Heisenberg operator equations that govern the atom's response to the incident laser field. We connect the Heisenberg variables with the notation used in RE. The method of solution is shown in the Appendix. Section IV is devoted to the simplest example of discrete-continuum excitation, in which the limit $q\rightarrow\infty$ allows the Fano profile to be replaced by a Lorentzian function. Explicit analytic expressions are given for the photoelectron spectrum as a function of laser intensity (or, more conveniently, transition Rabi frequency[10]), laser detuning, and off-diagonal relaxation rate. A complex "level-shift" formula is obtained in closed form, in terms of which spectral peaks and widths can be easily determined.

Section V addresses the finite-q model. We show that it is still possible to give explicit analytic expressions for the photoelectron spectrum, and we obtain the most general complex level-shift formula in this case. The spectral line shape shows significant redistributive effects for large values of the off-diagonal relaxation rate. We identify a symmetry property of the spectrum, involving the exchange of elastic and inelastic peaks. We discuss the effect of relaxation on the confluence of coherences mentioned in RE, and identify the Rabi frequency as well as the ac Stark shifts associated with Autler-Townes[11] line splitting. In Sec. VI we summarize our findings briefly. Discussion of time-dependent effects, such as population trapping,[2–4,7] and the consideration of another relaxation model, are deferred to subsequent papers.

II. DESCRIPTION OF MODEL

In Fig. 1 we show the atomic model we will discuss. It is similar to the simplest model adopted by Fano in his discussion of autoionization in 1961.[1] It is characterized by three matrix elements

$$V_{01}=\langle 0\,|\,\hat{V}_{\rm rad}\,|\,1\rangle\ , \tag{2.1}$$

$$V_0(\omega)=\langle 0\,|\,\hat{V}_{\rm rad}\,|\,\omega\rangle\ , \tag{2.2}$$

$$V_1(\omega)=\langle 1\,|\,\hat{V}_{\rm Coul}\,|\,\omega\rangle\ , \tag{2.3}$$

where $V_{\rm rad}=[-\vec{d}\cdot\vec{E}_L(t)]_{\rm RWA}$ is the radiative dipole interaction energy in the rotating-wave approximation,[10] and $\hat{V}_{\rm Coul}$ is any (typically Coulombic, but see Ref. 7) configuration-mixing interaction energy that couples the discrete state $|1\rangle$ with the continuum $|\omega\rangle$. Here we have used a circumflex to designate atomic operators. The laser field $\vec{E}_L(t)$ will be treated classically, and ω_L is the laser photon frequency.

The Hamiltonian for the model can be written (with $\hbar=1$)

$$\hat{H}=\hat{H}_0+\hat{H}_1+\hat{H}_\omega+\hat{V}_{\rm Coul}+\hat{V}_{\rm rad}\ , \tag{2.4}$$

where the bare energies are given by

$$\hat{H}_0=E_0\,|\,0\rangle\langle 0\,|\ , \tag{2.5a}$$

$$\hat{H}_1=E_1\,|\,1\rangle\langle 1\,|\ , \tag{2.5b}$$

$$\hat{H}_\omega=\int d\omega\,\omega\,|\,\omega\rangle\langle\omega\,|\ . \tag{2.5c}$$

Following Fano, we begin by diagonalizing $\hat{H}_{1\omega C}=\hat{H}_1+\hat{H}_\omega+\hat{V}_{\rm Coul}$ and we denote the eigenvectors of $\hat{H}_{1\omega C}$ by round brackets. That is,

$$\hat{H}_{1\omega C}\,|\,\omega)=\omega\,|\,\omega)\ . \tag{2.6}$$

The new eigenbasis fully accounts for the finite lifetime of state $|1\rangle$ due to autoionization via the

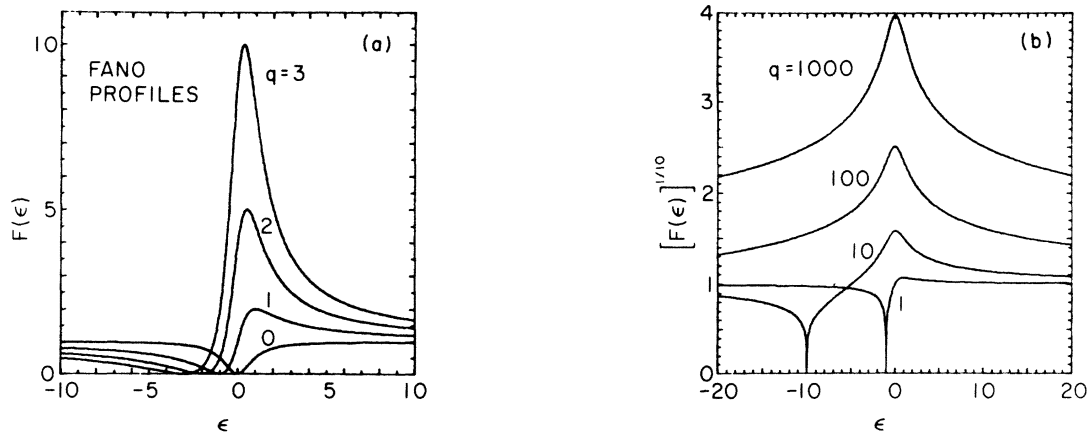

FIG. 2. (a) Plots of $F(\epsilon)$, given in Eq. (2.10), for several values of the asymmetry parameter q showing the Fano zeros at $\epsilon=-q$. (b) Plots of $[F(\epsilon)]^{0.1}$ for a much greater range of q values. The line becomes a Lorentzian curve centered at $\epsilon=0$ as $q\rightarrow\infty$. Numerical enhancement via the very small exponent 0.1 is used to bring all four curves into approximately the same scale and to emphasize the zeros at $\epsilon=-1$ and -10.

Coulombic configuration-mixing interaction. We can express the radiative energy in terms of the new eigenbasis vectors:

$$\hat{V}_{\rm rad}=\int d\omega\,\Omega_\omega\,|0\rangle\langle\omega|+\text{H.c.}\,, \tag{2.7}$$

and the new bound-free radiative matrix element Ω_ω is given in terms of the old matrix element by

$$\Omega_\omega=V_0(\omega)e^{i\varphi}\frac{\epsilon(\omega)+q}{\epsilon(\omega)-i}\,. \tag{2.8}$$

Here φ is an arbitrary phase and q is the Fano asymmetry parameter that reflects the relative strength of radiative coupling between $|0\rangle$ and $|1\rangle$ compared to that between $|0\rangle$ and $|\omega\rangle$. As the direct bound-free coupling becomes relatively weaker, q becomes larger. Finally, $\epsilon(\omega)$ is Fano's dimensionless reduced energy

$$\epsilon(\omega)=[\omega-\omega_{10}-\mu(\omega)]/\gamma_1\,, \tag{2.9a}$$

where $\omega_{10}=E_1-E_0$ is the discrete-discrete transition energy, $\mu(\omega)$ is a small energy shift which we will ignore, and $(2\gamma_1)^{-1}$ is the lifetime for autoionization of state $|1\rangle$ into the continuum due to $\hat{V}_{\rm Coul}$:

$$2\gamma_1=2\pi\,|V_1(\omega)|^2\,. \tag{2.9b}$$

That is, the autoionization linewidth (half-width at half maximum) is γ_1. The bare density of continuum states has been taken to be unity; i.e., $\langle\omega|\omega'\rangle=\delta(\omega-\omega')$. As (2.8) and (2.9a) indicate, γ_1 sets the scale for structure in the continuum arising from the configuration mixing.

For later reference we remind the reader of one of Fano's main findings. The absolute square of the radiative matrix element $|\Omega_\omega|^2$ is essentially the linear weak-laser absorption cross section for photons of frequency ω. It is usually assumed that $V_0(\omega)$ is relatively insensitive to changes in ω. Thus the shape of the absorption line comes from the final factor $(\epsilon+q)/(\epsilon-i)$. We plot the square of this factor, the "Fano profile" $F(\epsilon)$ where

$$F(\epsilon)=(\epsilon+q)^2/(\epsilon^2+1)\,, \tag{2.10}$$

as a function of ϵ for several q values in Fig. 2. Note that each curve has a zero at $\epsilon=-q$ and a peak at $\epsilon=1/q$. The zero arises from complete destructive interference between the two ionization channels open to an electron in state $|0\rangle$. When the photon field is sufficiently strong, photoabsorption is no longer well described by the cross section plotted in Fig. 2. Nevertheless, both the peak and the zero in the Fano profile continue to have a strong influence on the laser-atom interaction. We will return to this point later.

It is obvious that (2.8) can be rewritten

$$\Omega_\omega=\frac{\Omega_0}{\sqrt{4\pi\gamma_1}}\left[\frac{1}{\epsilon-i}+\frac{1}{q+i}\right], \tag{2.11}$$

where we have identified the Rabi frequency[10] of the interaction:

$$\Omega_0\equiv\sqrt{4\pi\gamma_1}(q+i)V_0(\omega)e^{i\varphi}\,. \tag{2.12}$$

By an appropriate choice of φ, Ω_0 is defined to be real. In (2.11) it is clear that Fano's model consists of the superposition of a Lorentzian resonance and a flat background. It will be useful to modify the model slightly by giving the flat background a finite width. This can be done in several ways. The most

convenient modification, from the standpoint of analytic simplicity of the final formulas, appears to be to turn the flat background into a very broad Lorentzian. Thus in our model we replace (2.11) with

$$\Omega_\omega=\frac{\Omega_0}{\sqrt{4\pi\gamma_1}}\left[\frac{1}{\epsilon-i}-\frac{1}{q+i}\frac{i\sigma}{\epsilon-i\sigma}\right] . \quad (2.13)$$

This can be called a two-Lorentzian model for autoionization. Note that the sign of σ has been changed relative to that of RE, but we will take the limit $\sigma\to\infty$, where the difference is clearly insignificant.

We have presented in RE some of the principal results of an analysis of the radiative phenomena associated with the two-Lorentzian Fano-type model described here. These include broadening and narrowing and splitting of the free-photoelectron spectrum under various conditions, and a certain confluence of bound-free coherences. These phenomena are related to those we discuss below, and we will recall them later at the appropriate places in our analysis.

III. PHASE INCOHERENCE

In this section we add a new feature to the two-Lorentzian model. We assume the existence of atomic dipole phase diffusion in order to study the effect of phase incoherence on autoionization. One can say that the phase incoherence arises, for example, because the exciting laser is not perfectly monochromatic, or because the atom is subject to random weak elastic collisions. In any event, the incoherence that we introduce in this section is off-diagonal (or transverse, in the sense of optical resonance[10]). It has no effect on excited-state lifetimes, but causes line broadening in absorption. Thus it is physically distinct from the incoherence arising from finite lifetimes discussed by Agarwal *et al.*[4]

We will use the Wiener-Levy description of phase diffusion[12] for definiteness. If we denote by $\psi(t)$ the phase of the atomic dipole moment relative to the laser field, then $\psi(t)$ is a Gaussian stochastic process, and the instantaneous frequency deviation is delta correlated:

$$\langle\langle\dot{\psi}(t_1)\dot{\psi}(t_2)\rangle\rangle=2\gamma_T\delta(t_1-t_2) . \quad (3.1)$$

Here the double angle bracket indicates an average over the statistical ensemble, and γ_T is the (transverse) coherence time associated with the phase diffusion. It is well known that Wiener-Levy phase diffusion is associated with Lorentzian spectral line shapes,[13] which do not describe accurately either collisional or laser broadening very far from line center. Thus we must restrict our attention to cases where ω_L is not many times γ_T away from line center (nominally located at $\omega_{10}=E_1-E_0$).

The Hamiltonian for the model, in the presence of transverse incoherence, is the same as before except for the following replacement in (2.7):

$$\Omega_\omega\to\Omega_\omega e^{+i\psi(t)} . \quad (3.2)$$

In other words, we can write, in the rotating coordinate frame,

$$\hat{H}=E_0|0\rangle\langle 0|+\int d\omega\,\omega|\omega)(\omega| + \int d\omega\,\Omega_\omega e^{+i\psi(t)}|0\rangle(\omega|+\text{H.c.} \quad (3.3)$$

Note that the round bracket states, which include the original discrete excited state $|1\rangle$, are used here. The Hamiltonian given in (3.3) is exact in the dipole and rotating-wave approximations. We will simplify some of the algebra later by choosing $E_0=0$. Recall that, although E_1-E_0 is not apparent in (3.3), it is contained in Ω_ω [see (2.13) and (2.9)].

The three principal atomic variables of the photoexcitation process are

$$\hat{P}_0=|0\rangle\langle 0| , \quad (3.4a)$$

$$\hat{B}_\omega=|0\rangle(\omega|e^{i\psi(t)} , \quad (3.4b)$$

$$\hat{C}_{\omega\omega'}=|\omega)(\omega'| . \quad (3.4c)$$

We will designate quantum expectation values simply by removing the circumflex. That is, for any operator $\hat{A}$ we have

$$A\equiv\langle\hat{A}\rangle\equiv\text{Tr}\{\hat{\rho}\hat{A}\} , \quad (3.5)$$

where $\hat{\rho}$ is the atomic density operator.

Expectation values allow direct contact with the formalism used in RE as follows. If the atomic evolution can be described with pure states, then the density operator remains a projection operator for all time. In the Schrödinger picture one then has

$$\hat{\rho}(t)=|\Psi(t)\rangle\langle\Psi(t)| , \quad (3.6)$$

and the exact state function can be written as

$$|\Psi(t)\rangle=\alpha(t)|0\rangle+\int d\omega\,\beta_\omega(t)|\omega) . \quad (3.7)$$

The pure-state amplitudes $\alpha(t)$ and $\beta_\omega(t)$ were used in RE, and a similar approach based on state amplitudes was followed by Lambropoulos and Zoller[3] and by Coleman and Knight.[7] The connections with Eqs. (3.4) are as follows [recalling (3.5)]:

$$|\alpha(t)|^2=P_0(t) , \quad (3.8a)$$

$$\alpha^*(t)\beta_\omega(t)=B_\omega(t)e^{-i\psi(t)} , \quad (3.8b)$$

$$\beta^*_\omega(t)\beta_{\omega'}(t)=C_{\omega\omega'}(t) . \quad (3.8c)$$

In contrast to RE, and to Refs. 3 and 7, we cannot here assume that our atom-laser interaction per-

mits a pure-state description. This is because of the "collisional" relaxation effects introduced by the random phase $\psi(t)$. The consideration of radiative relaxation effects also generally prevents a pure-state description. Nevertheless, Eqs. (3.8) guide our interpretation of the dynamical variables. For example, we note that $P_0(t)$ is the population of the ground state, and $C_{\omega\omega}(t)$ is the probability (per unit frequency) that the electron has energy ω.

The relevant equations for the dynamical variables are easily found in the Heisenberg picture, using obvious elementary commutators. For examples, we have

$$[\,|0\rangle\langle 0|\,,|0\rangle\langle\omega|\,]=|0\rangle\langle\omega|\,, \tag{3.9a}$$

$$[\,|0\rangle\langle\omega|\,,|\omega'\rangle\langle\omega|\,]=|0\rangle\langle\omega|\delta(\omega-\omega')\,. \tag{3.9b}$$

Heisenberg's equation of motion $i\partial/\partial t=[\,,\hat{H}]$ leads to the following dynamical equations, which must be solved:

$$\partial\hat{P}_0/\partial t=-i\int d\omega\,\Omega_\omega\hat{B}_\omega+\text{H.c.}\,, \tag{3.10a}$$

$$\partial\hat{B}_\omega/\partial t=-i(\omega-\omega_L-\dot{\psi})\hat{B}_\omega-i\Omega_\omega^*\hat{P}_0 +i\int d\omega'\Omega_{\omega'}\hat{C}_{\omega\omega'}\,, \tag{3.10b}$$

$$\partial\hat{C}_{\omega\omega'}/\partial t=i(\omega-\omega')\hat{C}_{\omega\omega'}-i\Omega_\omega^*\hat{B}_\omega^\dagger +i\Omega_\omega\hat{B}_\omega\,. \tag{3.10c}$$

Notice that $\hat{C}_{\omega\omega'}$ is not subject to the relaxation process $\dot{\psi}$ directly. This is obvious in the case of laser phase diffusion. It is also true in the case of collisional dephasing when collisions act to shift all continuum levels equally, which we assume.

Equations (3.10a)–(3.10c) are stochastic integrodifferential equations. They are exactly solvable under the conditions of our model. The solutions have two complementary aspects, temporal and spectral. We will deal here with the spectral aspects, and describe the predicted spectrum of electrons in the state $|\omega)$. The relevant solutions are obtained by a method explained in the Appendix. Sections IV and V deal with the results appropriate to symmetric ($q\to\infty$) and asymmetric (finite-q) Lorentzian models, respectively.

IV. PHOTOELECTRON SPECTRUM, ONE-LORENTZIAN CONTINUUM

We first discuss the one-Lorentzian case, in effect taking the limit $q\to\infty$ while holding Ω_0 fixed, so that

$$|\Omega_\omega|^2=\frac{\Omega_0^2}{4}\frac{\gamma_1/\pi}{(\omega-\omega_{10})^2+\gamma_1^2}\,. \tag{4.1}$$

In Sec. V we examine the same problem for finite values of q.

It might be thought that the one-Lorentzian model offers little of interest.[13] It is easy to verify that formula (4.1) is identical to $1/\pi$ times the photon absorption rate of a two-level system with transition frequency ω_{10} and upper-state lifetime $(2\gamma_1)^{-1}$ exposed to incident photons with energy ω and Rabi frequency Ω_0. However, the Lorentzian form of (4.1) is not enough to make this the same problem as absorption by a lifetime-broadened two-level atom. We note that, in a certain sense, the one-Lorentzian continuum model has no broadening at all. That is, each state $|\omega)$ is an exact eigenstate of $\hat{H}_0+\hat{H}_1+\hat{H}_\omega+\hat{V}_{\text{Coul}}$ with zero decay rate. The parameter γ_1 has a structural, but not a dynamic significance in the $|\omega)$ basis.

The analogy with a simple two-level system is in some respects misleading. The one-Lorentzian continuum problem has three independent energies: the 0-1 transition energy ω_{10}, the incident photon energy ω_L, and the photoelectron energy ω. In this respect the photoionization process considered here is closer to the more complex two-photon process of stimulated Raman scattering.[14] The latter analogy has been noted by Knight[15] in the case of a nonresonant infinitely broad continuum. The connection with double–optical-resonance phenomena in general was made by Lambropoulos and Zoller[3] and by Andryushin *et al.*[6]

In this section we use the one-Lorentzian continuum to explain the features of autoionization that do *not* depend on Fano-type interferences. We do this by focusing our attention on the long-time probability that an electron is in state $|\omega)$. We will call this quantity the photoelectron spectrum $W(\omega)$;

$$W(\omega)=\lim_{t\to\infty}C_{\omega\omega}(t)\,. \tag{4.2}$$

Our model allows $W(\omega)$ to be computed directly and completely analytically, in a form that, in many respects, can be interpreted by inspection. The method is given in the Appendix. The result is

$$\pi W(\omega)=\frac{\Delta^2(\gamma_1\gamma_T/\gamma)+\gamma(\gamma_1\gamma_T+\Omega_0^2/4)}{[\delta(\delta-\Delta)-\gamma_1\gamma_T-\Omega_0^2/4]^2+(\delta\gamma-\Delta\gamma_T)^2}\,, \tag{4.3}$$

where δ is the "inelasticity" of the ionized electrons of frequency ω,

$$\delta\equiv\omega-\omega_L\,; \tag{4.4a}$$

and Δ is the usual detuning of the laser from the absorption line,

$$\Delta=\omega_{10}-\omega_L\,; \tag{4.4b}$$

and γ is the sum of linewidths,

$$\gamma=\gamma_1+\gamma_T \ . \tag{4.4c}$$

Equation (4.3) is the main result of Sec. IV. Its interpretation is greatly facilitated by the exact factorization of its denominator, which is possible for both $\gamma_T=0$ and $\gamma_T\neq 0$. We consider the two cases separately.

Case (i): Collisionless monochromatic excitation ($\gamma_T=0$). This case is familiar in the weak-field limit, but (4.3) is not restricted to weak fields (small Ω_0). The collisionless limit of (4.2) is the product of separate factors (see also the analysis in RE in the limit $q\rightarrow\infty$):

$$\pi W(\omega)=\gamma_1\frac{\Omega_0^2}{4}\,|\,\mathscr{L}_+(\delta)\mathscr{L}_-(\delta)\,|^2 \tag{4.5a}$$

with $\mathscr{L}_\pm$ denoting complex Lorentzian functions

$$\mathscr{L}_\pm(\delta)\equiv\frac{1}{\delta-\frac{1}{2}(\Delta\pm\Lambda+i\gamma_1)} \ , \tag{4.5b}$$

where Λ can be interpreted as a complex level shift

$$\Lambda=A+iB \ , \tag{4.6a}$$

$$A+iB=[(\Delta+i\gamma_1)^2+\Omega_0^2]^{1/2} \ . \tag{4.6b}$$

The structure of $A+iB$ indicates that our definition of Ω_0 in (2.12) has correctly identified it as the Rabi frequency when $q\rightarrow\infty$.

In the limit of a weak exciting field the two factors have a clear interpretation as "elastic" and "inelastic" spectra. To show this we take the limit $\Omega_0\rightarrow 0$, keeping only the first contribution dependent on Ω_0. We find

$$A\simeq\Delta+\frac{\Delta\Omega_0^2/2}{\Delta^2+\gamma_1^2} \ , \tag{4.7a}$$

$$B\simeq\gamma_1-\frac{\gamma_1\Omega_0^2/2}{\Delta^2+\gamma_1^2} \ , \tag{4.7b}$$

and so the two factors in (4.5) give rise to spectral peaks at $\delta\approx 0$ (i.e., $\omega\approx\omega_L$, elastic) and $\delta\approx\Delta$ (i.e., $\omega\approx\omega_1$, inelastic).

The weak-field widths and heights of the two peaks of $\pi W(\omega)$ for $\gamma_T=0$ are easily found to be the following. For the elastic peak, with width $w_{\rm el}$ and height $h_{\rm el}$,

$$w_{\rm el}=\gamma_1\Omega_0^2/4(\Delta^2+\gamma_1^2) \tag{4.8a}$$

and

$$h_{\rm el}=(w_{\rm el})^{-1} \ , \tag{4.8b}$$

and thus the elastic peak is purely power broadened, with approximately unit area. For the inelastic peak, with width $w_{\rm inel}$ and height $h_{\rm inel}$,

$$w_{\rm inel}=\gamma_1 \tag{4.9a}$$

and

$$h_{\rm inel}=\Omega_0^2/4\gamma_1\Delta^2\neq(w_{\rm inel})^{-1} \ . \tag{4.9b}$$

The inelastic peak is lifetime broadened, with negligible area. All of these features are shown in Fig. 3(a) where we have drawn $\log_{10}[(\pi/4)\Omega_0^2 W]$. The extra factor of Ω_0^2 normalizes the elastic peak heights to the same value, independent of Ω_0. Note the complete insignificance of the inelastic peaks. For the values of Ω_0 chosen, the elastic peak width is 1000 times narrower than the plotting grid and

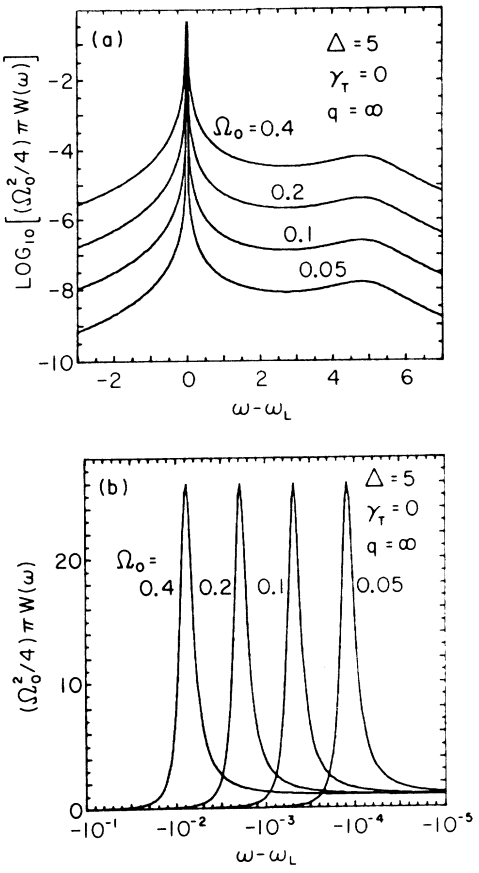

FIG. 3. (a) Plots of $\Omega_0^2/4$ times the scattered electron spectrum for four values of the Rabi frequency Ω_0. The logarithmic vertical scale allows the very weak inelastic peak to be seen. All of the stated parameter values are in units of the auto-ionization linewidth γ_1. That is, $\Omega_0=0.1$ means $\Omega_0=0.1\gamma_1$, and $\omega-\omega_L=2$ means $\omega-\omega_L=2\gamma_1$, etc. We will follow this convention throughout the paper. (b) A greatly expanded view of the elastic peaks of the spectra shown in (a). Peak heights and Stark shifts are in agreement with Eqs. (4.8a) and (4.8b), after account is taken of the logarithmic horizontal axis and the multiplication of the spectrum by $\Omega_0^2/4$.

the true peaks are skipped. These are shown in Fig. 3(b) on a greatly expanded frequency scale, which has enough resolution to show the small peak shift (the so-called ac Stark shift) given in Eq. (4.7a) as well.

In the case of higher laser power the dependence of various spectral features on Ω_0^2 is less simple than what is shown in Figs. 3(a) and 3(b). No scaling relations allow Ω_0 to be removed from $W(\omega)$ completely, and the intrinsic spectral shape changes with Ω_0. This is shown in Fig. 4 where Ω_0^2 varies over four orders of magnitude altogether. Both detuning Δ and inelasticity δ are scaled to $\Omega_0/2$, and the spectrum itself is scaled as in Figs. 3(a) and (3b). Nevertheless, the character of the spectrum changes dramatically. It is no longer accurate to identify the two peaks with elastic and inelastic scattering processes. One notes that the positions of the peaks shift as a function of Ω_0. Even on the scaled axis, where $x=(\omega-\omega_L)/(\frac{1}{2}\Omega_0)$, the peaks shift from their purely elastic and inelastic positions 0 and 2 to $1-\sqrt{2}$ and $1+\sqrt{2}$.

In Fig. 5 the progressive splitting is shown against an unscaled axis. The weak-field curve shows a familiar strong preference for elastic scattering. Its peak at $\omega=\omega_L$ is approximately three orders of magnitude higher than the peak at $\omega-\omega_L=\Delta$ (i.e., at $\omega=\omega_1$). However, an increase of Ω_0 from $\Omega_0=1$ to 8 (we will consistently quote numerical values in units of the autoionization width γ_1) is sufficient to split the spectral peaks by a factor of 4 times their weak-field splitting, and to bring the inelastic peak almost to parity with the elastic peak. This is nothing but the appearance of the Autler-Townes effect,[11] normally associated with radiative probes of discrete two-level systems, in the electron spectrum.[16] It is well known in the case of discrete-discrete transitions that for $\Omega_0 \gg \Delta, \gamma_1$ the two Autler-Townes peaks are split by $(\Omega_0^2+\Delta^2)^{1/2}$ and are symmetrically located on either side of $\delta=\pm\frac{1}{2}\Delta$. They have a width determined by the "probe" used to observe them. Here we see the same features, even though the upper state is continuous, not discrete. In this case the "probe" is Coulombic leakage from $|1\rangle$ to $|\omega\rangle$ here, so the width is γ_1. All of these features are evident in Fig. 5.

Case (ii): With collisions and/or finite laser bandwidth ($\gamma_T \neq 0$). A pure-state analysis is no longer possible, and the results of RE are not useful. However, we can again factor the denominator of the spectrum and so can still describe the results in terms of an elastic and an inelastic peak. In this case we find

$$\pi W(\omega)=\frac{(\Delta^2+\gamma^2)\left[\frac{\Omega_0^2}{4}\frac{\gamma}{\Delta^2+\gamma^2}+\frac{\gamma_1\gamma_T}{\gamma}\right]}{\left[\left[\delta-\frac{\Delta-A_T}{2}\right]^2+\left[\frac{\gamma-B_T}{2}\right]^2\right]\left[\left[\delta-\frac{\Delta+A_T}{2}\right]^2+\left[\frac{\gamma+B_T}{2}\right]^2\right]} . \tag{4.10}$$

Again there is a complex level shift

$$\Lambda_T=A_T+iB_T \tag{4.11a}$$

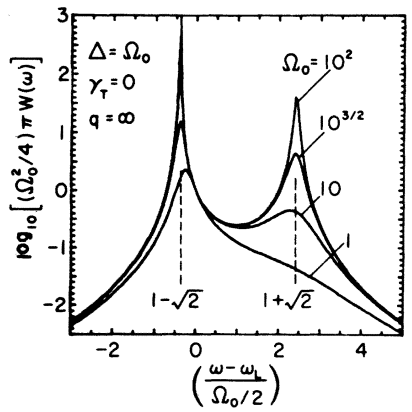

FIG. 4. Plots of $\Omega_0^2/4$ times the electron spectrum shown on a scaled frequency axis: $x=(\omega-\omega_L)/(\frac{1}{2}\Omega_0)$. Note the fixed point at $\omega=\omega_L$ for all values of Ω_0. The height of the highest left-hand peak is 3.16.

and A_T and B_T are only slightly different from A and B given in (4.6):

$$A_T+iB_T=\{[\Delta+i(\gamma_1-\gamma_T)]^2+\Omega_0^2\}^{1/2} . \tag{4.11b}$$

Also, γ is the sum of autoionizing and transverse widths:

$$\gamma=\gamma_1+\gamma_T . \tag{4.12}$$

Note that in the definition of A_T+iB_T we find $\gamma_1-\gamma_T$ instead of $\gamma_1+\gamma_T$. This is an indication of coherent transient interference in the autoionization process by the laser signal. In the present context it is a strong-field effect. The weak-field limit of (4.10) is interesting because it shows not only that all dependences on the difference $\gamma_1-\gamma_T$ vanish, but also makes clear our earlier remark about the similarity of the present problem to resonance fluorescence and Raman scattering. In particular, one finds, as $\Omega_0 \to 0$ that (4.10) predicts

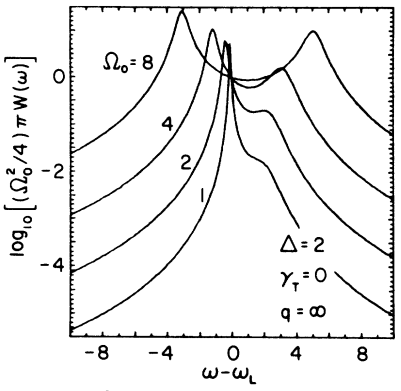

FIG. 5. Plots of the electron spectrum, showing increasingly significant Autler-Townes splitting as Ω_0 increases from 1 to 8. Note the same fixed point as in Fig. 4.

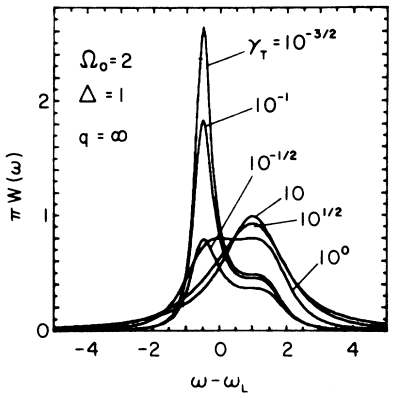

FIG. 6. Plots of the electron spectrum, showing the significance of transverse relaxation in determining spectral line shape. Note the spectral symmetry for $\gamma_T=\gamma_1$ $(=1.0)$.

$$\pi W(\omega)\rightarrow \frac{\frac{\gamma_1\gamma_T}{\gamma_1+\gamma_T}(\Delta^2+\gamma^2)}{[(\omega-\omega_{10})^2+\gamma_1^2][(\omega-\omega_L)^2+\gamma_T^2]} . \quad (4.13)$$

This is *exactly* the expression one obtains when the weak-field resonance fluorescence spectrum of Knight *et al.*[17] is normalized to unity (and thereby made independent of Ω_0, incidentally). This can be seen most directly by comparison with Eq. (13) of Raymer and Cooper.[17] As in the "collisionless" case discussed above, the weak-field heights and widths of the elastic and inelastic peaks are easily obtained. In the weak-field limit, expression (4.10) reduces to a sum of two Lorentzian peaks if $\Delta \gg \gamma$. The scattering strengths of these two peaks then satisfy a simple sum rule. If we denote by $S_{\rm el}$ and $S_{\rm inel}$ the areas of the separate peaks, then we can write

$$S_{\rm el}\simeq\gamma_1/\gamma,\quad S_{\rm inel}\simeq\gamma_T/\gamma \quad (4.14a)$$

or

$$S_{\rm el}+S_{\rm inel}=1 . \quad (4.14b)$$

In strong contrast to the collisionless case, here the inelastic scattering strength is significant if γ_T is an appreciable fraction of γ_1, even for weak fields, and may even be larger than the elastic scattering strength. The inelastic electron peak has an origin quite similar to that of the collisionally assisted fluorescence studied recently by Raymer *et al.*,[18] and is an example of spectral redistribution[9] in scattering. Figure 6 shows how dramatically an increase in collisional assistance (increase in γ_T) can affect spectral redistribution. Both the position and shape of the spectrum are grossly changed. In contrast, relaxation due to finite level lifetimes, for example radiative relaxation,[4] does not give rise to spectral redistribution.

For moderate or strong fields the spectrum can be completely different, and the clear distinction between elastic and inelastic effects can be lost. Exactly resonant excitation ($\Delta=0$) gives a case of some interest, because we then have

$$A_T+iB_T\rightarrow[\Omega_0^2-(\gamma_1-\gamma_T)^2]^{1/2} . \quad (4.15)$$

This implies that one of A_T and B_T *must vanish,* depending on the size of Ω_0 relative to the difference $\gamma_1-\gamma_T$. If B_T vanishes, the spectrum has two peaks located at

$$\delta_\pm=\pm\tfrac{1}{2}A_T \quad (4.16)$$

and they both have half-width γ_1. The spectrum has the pure Autler-Townes form if $\Omega_0 \gg |\gamma_1-\gamma_T|$.

On the other hand, if A_T vanishes, the spectrum has a single peak located at $\delta=0$, and this single peak has two widths:

$$\gamma_\pm=\tfrac{1}{2}|\gamma\pm B_T| . \quad (4.17)$$

[In the low-power limit these widths are just γ_1 and γ_T, as in (4.13) for $\omega_L=\omega_1$.] Figure 7 shows the details of the transition between the one-peaked and two-peaked forms at resonance.

According to these remarks, $W(\omega)$ is unaffected, at resonance, by the exchange of γ_1 and γ_T. This is only part of a more general symmetry in the spectrum. $W(\omega)$ is also invariant under the double exchange $(\omega_1,\gamma_1)\leftrightarrow(\omega_L,\gamma_T)$. Thus, for example, in Figs. 6 and 8 the curve labeled $\gamma_T=1$ (numerical values in units of γ_1) is completely symmetric about $\delta=0.5$ and 2.0, respectively, namely, symmetric about $\delta=\Delta/2$ in both cases.

There is a well-defined limit of $W(\omega)$ for very large γ_T. We find, when γ_T is large enough,

$$\pi W(\omega)=\frac{\gamma_1}{(\omega-\omega_1)^2+\gamma_1^2} . \quad (4.18)$$

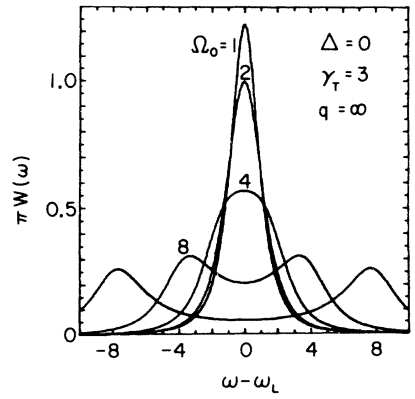

FIG. 7. Plots of the electron spectrum, showing the transition from one-peak (weak-field) to two-peak (Autler-Townes) line shapes.

In other words, the electron spectrum becomes entirely inelastic and completely insensitive to the details of the light line shape as long as the light bandwidth is large enough. The shape of the electron spectrum comes to reflect only the structure of the continuum if $\gamma_T \gg \Omega_0, \Delta, \gamma_1$. This is shown most clearly in Fig. 8 where both $\gamma_T = 100$ and $\gamma_T = 1000$ are sufficiently large, and so give very similar, nearly Lorentzian, spectra with half-widths of 1.0.

Equation (4.18) shows plainly the normalization adopted for the spectrum, namely,

$$\int_{-\infty}^{\infty} W(\omega) d\omega = 1 \,. \tag{4.19}$$

This is because our spectrum is defined in the very long-time limit. All bound-state electrons are eventually ionized, with unit probability and independent of laser power. Only the spectral distribution of electrons is influenced by Ω_0. This is not at all true for short times, as Lambropoulos and Zoller[3] have

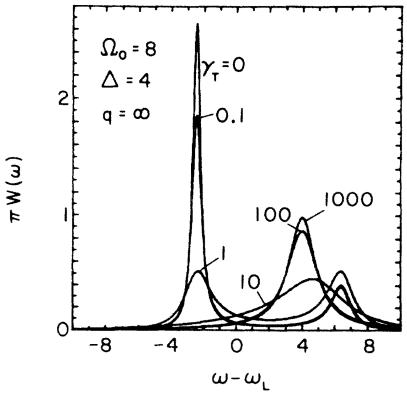

FIG. 8. Plots of the electron spectrum, showing spectral redistribution as the transverse relaxation rate is increased. Asymptotic Lorentzian shape is approached by the curves for $\gamma_T = 100$ and 1000.

shown when $\gamma_T = 0$; and it is not true for finite q if Ω_0 is properly adjusted. We will discuss time dependences in another paper.[19]

The nature of the spectrum for high laser power has already been discussed for $\gamma_T = 0$. There are very minor high-power differences when $\gamma_T \neq 0$. In the generalized high-power limit defined by

$$(\Omega_0^2 + \Delta^2)^{1/2} \gg \gamma_1, \gamma_T \tag{4.20}$$

there are spectral peaks located at $\delta = \delta_\pm$, where

$$\delta_\pm = \tfrac{1}{2}[\Delta \pm (\Omega_0^2 + \Delta^2)^{1/2}] \,, \tag{4.21}$$

and they have the same width, $\frac{1}{2}(\gamma_1 + \gamma_T)$, and height. Since the peak splitting is just $(\Omega_0^2 + \Delta^2)^{1/2}$ the definition of the high-power limit ensures that the two peaks are distinct from each other. Just as in the monochromatic case, this can be called the pure Autler-Townes[11] region of power dependence.

Finally, we recall our remarks in Sec. I. The existence of Autler-Townes spectral features is evidence for the repeated coherent continuum-to-discrete electronic recombination mentioned there. The generalized level-shift formula (4.11b) contains the criterion for such recombination, and it is the same as (4.20). That is, condition (4.20) guarantees that a fraction of the electronic probability oscillates between states $|0\rangle$ and $|\omega)$. If $\Omega_0 \gg \Delta$, this fraction can be significant. We emphasize the coherent aspect of such probability oscillation (Rabi oscillation) and caution the reader that it is quite different from inverse bremsstrahlung or other incoherent recombination processes. Graphs of coherent recombination versus time were shown in RE and in Refs. 3 and 7.

V. PHOTOELECTRON SPECTRUM, FANO-SHAPE CONTINUUM

In this section we turn our attention to the two-Lorentzian, or extended Fano-shape, continuum. Recent experiments[20] have identified autoionizing states with low values of q, in the range $q \simeq 2-10$, for which the Fano asymmetry is significant. In this section we obtain the long-time spectrum of photoelectrons for such asymmetric cases. We continue to use the model given in (3.3) and (2.13), for which our equations (3.10) are exactly soluble for arbitrary q.

The integral equation (A.11) of the model, for arbitrary q, has the following kernel [see (A.12)]:

$$K_{\omega\omega''} = \frac{\mu_\sigma(z)}{(z + \gamma_\sigma - i\omega)(z + \gamma_\sigma - i\omega'')} + \frac{\mu_1(z)}{(z + \gamma_1 - i\omega)(z + \gamma_1 - i\omega'')} \,, \tag{5.1}$$

where $\gamma_\sigma \equiv \sigma\gamma_1$ and

$$\mu_1(z)=\frac{\Omega_0^2/4}{\mathscr{H}(z,-i\gamma_1)}\left[1-\frac{2\gamma_\sigma}{(1+iq)(\gamma_\sigma+\gamma_1)}\right] \tag{5.2a}$$

and

$$\mu_\sigma(z)=\frac{\Omega_0^2/4}{\mathscr{H}(z,-i\gamma_\sigma)} \times\left[\frac{\gamma_\sigma}{\gamma_1(1+q^2)}-\frac{2\gamma_\sigma}{(1-iq)(\gamma_\sigma-\gamma_1)}\right] \tag{5.2b}$$

and $\mathscr{H}(z,\omega)$ is still defined by (A.10) with (2.13) used for Ω_ω. The obvious strategy, therefore, is to solve first for

$$A_\sigma=\int d\omega'\frac{D^\dagger_{\omega'}}{z+\gamma_\sigma-i\omega'}\ , \qquad A_1=\int d\omega'\frac{D^\dagger_{\omega'}}{z+\gamma_1-i\omega'}\ , \tag{5.3}$$

and later for $D_{\omega'}$. These tedious calculations lead to an explicit expression for the electron's spectrum.

We give first the formula for the spectrum in the collisionless case (when it can also be derived straightforwardly as explained in RE). The collisionless spectrum (normalized to unit area) reads

$$\pi W(\omega)=[\Omega_0^2/4(1+q^2)\gamma_1 P(\omega,q)]\{[(\delta-\Delta)(\gamma_1+\gamma_\sigma)+q\gamma_1\gamma_\sigma]^2+[(\delta-\Delta)q\gamma_1]^2\}\ , \tag{5.4}$$

where the denominator polynomial is given by

$$P(\omega,q)=\left[\delta(\delta-\Delta)(\gamma_1+\gamma_\sigma)-\frac{\Omega_0^2}{4}\frac{q^2\gamma_1\gamma_\sigma}{(1+q^2)\gamma_1}\right] + \left[\delta[(\delta-\Delta)^2-\gamma_1\gamma_\sigma]-\frac{\Omega_0^2}{4(1+q^2)\gamma_1}\{(\delta-\Delta)[\gamma_\sigma+(1+q^2)\gamma_1]+2q\gamma_1\gamma_\sigma\}\right]\ . \tag{5.5}$$

The issue of finite-q autoionization is most easily addressed in the limit $\sigma\to\infty$, in which case the atom under discussion is exactly Fano's model, a single Lorentzian and a flat continuum. It is that case which we will discuss further. For finite γ_T our stochastic equations give the following exact expression for the spectrum of photoelectrons:

$$\pi W(\omega)=w_q\left[1+\frac{2\gamma_T S_3}{M(0)}\right]\left|\frac{\delta-\Delta+q\gamma_1}{z_+z_-}\right|^2\ . \tag{5.6}$$

Here δ and Δ are again given by (4.4a) and (4.4b) and the other symbols have the following definitions:

$$M(0)=(a_0-a_0^*)^2+2w_qS_3 +2\gamma_1(a_0b_0+a_0^*b_0^*)\ , \tag{5.7}$$

$$S_3=2\gamma_1|b_0|^2+a_0b_0^*+a_0^*b_0\ , \tag{5.8}$$

$$z_\pm=\delta-\tfrac{1}{2}[\Delta\pm L_q+i(\gamma+w_q)]\ , \tag{5.9}$$

where we have introduced

$$w_q=\Omega_0^2/4(1+q^2)\gamma_1 \tag{5.10}$$

which has a direct physical meaning as linewidth for very large Ω_0, and

$$a_0=w_q\gamma_1(q+i)^2\ , \tag{5.11}$$

$$b_0=i\Delta+\gamma+w_q\ . \tag{5.12}$$

Again γ is the sum of autoionization width and collision width, $\gamma=\gamma_1+\gamma_T$, and now L_q is the generalization of the complex level shifts given in (4.6) and (4.11):

$$L_q=\mathscr{A}+i\mathscr{B}\ , \tag{5.13a}$$

$$\mathscr{A}+i\mathscr{B}=\{[\Delta+i(\gamma_1-\gamma_T-w_q)]^2+4w_q\gamma_1(q+i)^2\}^{1/2}\ . \tag{5.13b}$$

It is easy to establish the validity of the limits:

$$L_q\underset{q\to\infty}{\to}\Lambda_T\underset{\gamma_T\to0}{\to}\Lambda\ . \tag{5.14}$$

The form of $W(\omega)$ given in (5.6) is surprisingly compact and does not appear to have been anticipated, even in earlier related studies[14] in the much simpler limit $q\to\infty$. The significance of (5.6) is not just that the spectrum is basically Lorentzian, but that the degree of interference of the Lorentzians (which is contained in the δ dependence of the numerator) is simple, even in the strong-field limit. Obviously $W(\omega)$ has two peaks, located at

$$\delta_\pm=\tfrac{1}{2}(\Delta\pm\mathscr{A})\ , \tag{5.15}$$

and these peaks will have widths given by

$$\gamma_\pm=\tfrac{1}{2}(\gamma+w_q\pm\mathscr{B})\ . \tag{5.16}$$

However, in contrast to (4.5) and (4.10), there is a nontrivial δ dependence in the numerator of (5.4)

and (5.6). This arises from the interference of the two channels in the Fano model. Remarkably enough, the only evidence in the shape of $W(\omega)$ for this interference is a zero in the photoelectron spectrum at $\delta=\Delta-q\gamma_1$, i.e., at $\omega=\omega_{10}-q\gamma_1$. This is shown in Fig. 9 where we have plotted spectra for the same q values used in Fig. 2, and the curves are seen to have the same zeros. The curve shapes in Figs. 2 and 9 are different because the electron emission spectrum is shown here and the weak-field photon absorption spectrum is shown in Fig. 2.

Figure 10 demonstrates several additional features of finite-q spectra. First, the absence of transverse relaxation in Fig. 10 means that the linewidths are smaller compared with Fig. 9. Thus the same zero at $q=-2$ is present in the $\Omega_0=1$ curve as it was in Fig. 9 but is much less effective, because the spectrum is nearly zero at $q=-2$ anyhow. Nevertheless, the zero still causes a slight skewing of the line. Notice that the skewing is *toward* the zero, and is accompanied by a spectral peak *increase*. Neither of these effects would occur if the zero simply depressed the photoelectron probability in its vicinity. We can conclude that the zero is associated with quantum interferences among the electron's transition amplitudes. Note that the corresponding $\Omega_0=1$ curve for $q=100$ is completely symmetric. This is consistent with the results of Sec. IV, obtained in the limit $q\to\infty$.

The curves in Fig. 10 corresponding to $\Omega_0=3$ show a much greater difference from each other. The $q=100$ spectrum exhibits a normal symmetric Autler-Townes shape, familiar from Sec. IV. However, the $q=2$ spectrum is very sharply affected because one of the Autler-Townes peaks is very close to the zero. (Notice that the farther peak is also strongly affected, showing the internal coherence of the Autler-Townes effect.) The most extreme manifestation of this alteration occurs whenever one of the spectral peaks falls exactly on the zero. In RE we have termed this a confluence of coherences because the existence of the zero is a coherence effect,[1] and the existence of an Autler-Townes doublet is also a coherence effect.[11] Whenever such a confluence occurs, the spectral peak is infinitely high and narrow. The lifetime of one excitation channel is infinite, and a definite fraction of the atomic electrons is trapped in state $|0\rangle$. Coleman and Knight[7] have discussed trapping effects in detail, and show that the dynamics of the trapping depends on certain complex eigenfrequencies which can be identified as $iz_{\pm}$ given in (5.8), evaluated for $\gamma_T=0$.

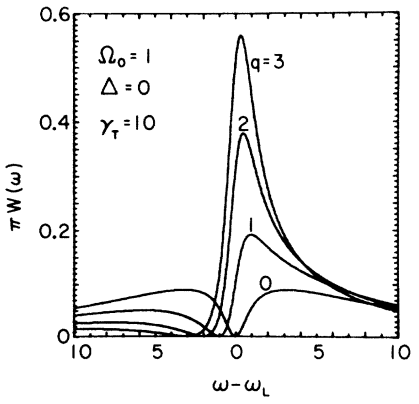

FIG. 9. Plots of the electron spectrum for several q values showing the same zeros as Fig. 2.

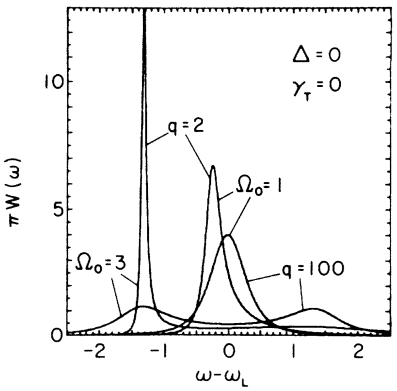

FIG. 10. Plots of the electron spectrum for high- and low-q values and for one-peak (weak-field) and two-peak (Autler-Townes) line shapes. Effect of the zero for $q=2$ is evident in both line shapes. Height of the narrowest peak is 12.8.

The exact conditions for confluence are easily derived by requiring that the zero in the numerator of (5.6) be counteracted by an identical zero in the denominator. This is the same as requiring

$$\delta-\tfrac{1}{2}[\Delta\pm L_q+i(\gamma+w_q)]=\delta-\Delta+q\gamma_1 \tag{5.17}$$

or

$$\pm L_q=\Delta-2q\gamma_1-i(\gamma+w_q)\,, \tag{5.18}$$

which yields the following equations for the real and imaginary parts of the square of (5.18):

$$w_q=\gamma_1-\Delta/q+\gamma_T\,, \tag{5.19}$$

$$w_q=\gamma_1-\Delta/q-\gamma_T/q^2\,. \tag{5.20}$$

These are obviously compatible only if $\gamma_T=0$, in which case the confluence condition can be written $\Omega_0=\Omega_c$, where

$$\Omega_c^2=4\gamma_1(1+q^2)(\gamma_1-\Delta/q)\,. \tag{5.21}$$

For $q=-1$ and $\Delta=\gamma_1$ this gives $\Omega_c=4\gamma_1$, as

predicted in RE.

It is easy to see that population trapping occurs at the confluence. To show this, and to determine the amount, it is sufficient to integrate $W(\omega)$ over all frequencies after imposing the confluence conditions $\gamma_T=0$ and $w_q=\gamma_1-\Delta/q$. The result, for the total probability of ionization is

$$\int W(\omega)d\omega=\frac{w_q}{\gamma_1+w_q} . \tag{5.22}$$

Thus the asymptotic un-ionized fraction is

$$P_0(\infty)=\frac{\gamma_1}{\gamma_1+w_q} , \tag{5.23}$$

which is in agreement with the corrected results of Ref. 7 and with Beers and Armstrong.[21]

The significance of the confluence is that it is the analog of the Fano zero in the extended model. That is, the existence of the zero in Fano's original model indicates that quantum interference may, for an appropriate choice of $\omega_{10}-\omega_L$, shut off the ground state from both of its ionization channels (direct and indirect). The confluence line narrowing shows that, no matter what choice is made for $\omega_{10}-\omega_L$, an appropriate choice of Ω_0 (i.e., of laser power) leads to a conspiracy of interferences with the same effect: The ground state cannot be completely ionized. (Obviously this conspiracy is impossible if $\omega_{10}-\omega_L>q\gamma_1$. We will discuss this and related points in detail elsewhere.[22])

It is important to observe that the presence of collisional incoherence (finite γ_T) does not eliminate the Fano zero in the spectrum. This is clear from expression (5.6), and is shown in Fig. 11, where three

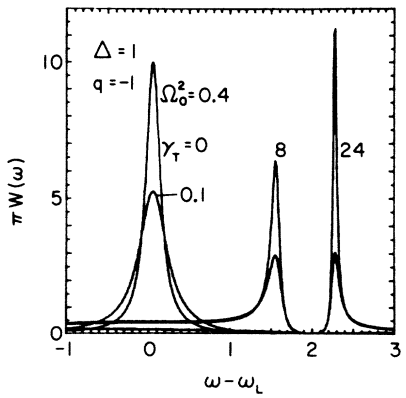

FIG. 11. Plots of the electron spectrum, showing three of the curves given in RE and in Ref. 4 to illustrate near-confluent line shapes for $\gamma_T=0$. Here the corresponding curves for $\gamma_T=0.1$ have been added. Note that the peak heights are suppressed, but the line shapes are unchanged. In contrast, see Figs. 12(b) and 12(d).

of the curves given in RE are reproduced for $\gamma_T=0$, and corresponding curves for $\gamma_T=0.1$ are added. It may at first be puzzling that a finite γ_T does not disrupt the exact destructive interference of the Fano calculation. However, it must be realized that the effect of dipole phase diffusion is exactly the same on both of the participating dipoles (both Heisenberg operators $|0\rangle\langle 1|$ and $|0\rangle\langle\omega|$) and so they do not accumulate any *relative* phase mismatch.[23]

On the other hand, there is an absolute effect on dipole coherence and, as a consequence, Autler-Townes interference is weakened. This manifests itself, for example, in the elimination of population trapping when $\gamma_T\neq 0$, which we will discuss elsewhere.[19] The Autler-Townes effect (which might be called "virtual" spectral redistribution) is also weakened by increasing γ_T in the sense that it gives way to real spectral redistribution. This redistribution is shown for strong and weak laser excitation and high- and low-q values in Fig. 12, and is similar to the redistribution discussed in Sec. IV.

The four graphs in Fig. 12 are designed to serve as summaries of the principle results obtained in the present work. These results are most clearly displayed for finite detuning, $\Delta=4$. Two of the graphs, Figs. 12(a) and 12(b), show our predictions for weak-field excitation. In the absence of collisional broadening they show extremely high elastic peaks with widths much less than γ_1. However, even a moderate amount of collisional relaxation, $\gamma_T=\gamma_1$, is sufficient to alter the spectral line shape dramatically. When $\gamma_T>\gamma_1$ there is nearly complete spectral redistribution. The peak of spectral response comes at $\omega=\omega_1$ (i.e., at $\delta=\Delta$) in that case, instead of at $\omega=\omega_L$ (i.e., at $\delta=0$).

The other two graphs, Figs. 12(c) and 12(d), show our predictions for strong-field excitation. There is noticeable Autler-Townes splitting for curves with $\Omega_0>\gamma_T$, and the same kind of spectral redistribution as in 12(a) and 12(b) occurs with $\Omega_0<\gamma_T$. For both strong and weak fields, the high-q curves, Figs. 12(a) and 12(c), show a good approximation to the spectral symmetry predicted for $\gamma_T=\gamma_1$ when $q\rightarrow\infty$. It should be noted that this is not pure Autler-Townes doublet symmetry, despite the equal heights and widths of the peaks. Finally, the low-q curves, Figs. 12(b) and 12(d), give striking evidence of the effects of the Fano zero on the spectral shapes. As we mentioned, even the spectra with large γ_T show exact zeros at $\delta=\Delta-q\gamma_1$. The shape distortions shown are all in the nature of a pulling toward the zero, rather than a simple suppression of probability in its vicinity.

When $\Delta=0$ there is, of course, no real redistribution since the elastic and inelastic peaks coincide.

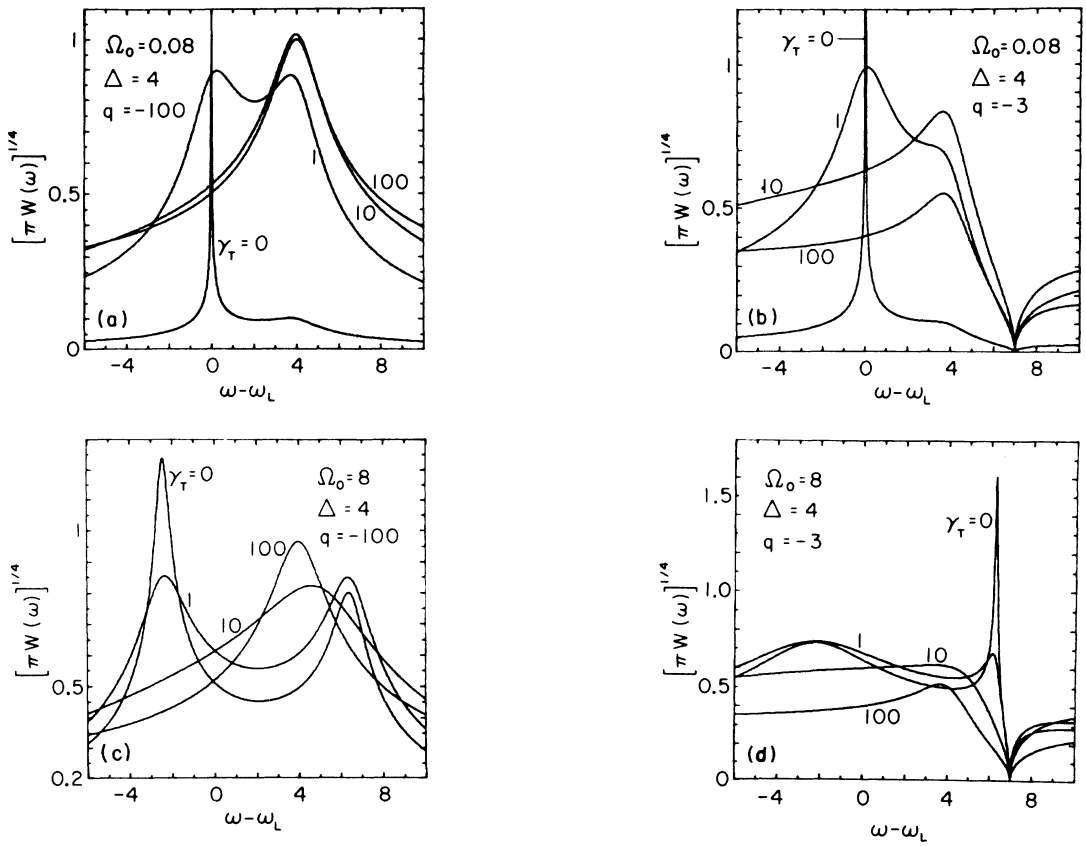

FIG. 12. Plots of the electron spectrum, showing the redistributive effect of large values of γ_T for both large and small q. Large q plots show evidence of the exact symmetry obtained for $\gamma_T=\gamma_1$ ($=1.0$) when $q\rightarrow\infty$. Weak-laser q plots have elastic peaks that far exceed the plot boundaries: in (a) the narrowest peak height is 9800, and in (b) it is 2168. Small-q plots show that the effects of the zero at $\omega-\omega_L=\Delta-q\gamma_1=7$ are much more pronounced for $\Omega_0=8$ because Ω_0 is close to the confluence value given by (5.21), $\Omega_c=[4\times10(1+4/3)]^{1/2}\approx9.7$.

Nevertheless, Autler-Townes splitting (virtual redistribution) may be present. In Fig. 13 we consider such a case because it allows another comparison with results of Agarwal *et al.*, shown in their curve labeled $\Omega=0.1$ (i.e., $\Omega_0^2=40.4$ according to the summary of parameter translations given below) in Fig. 3 of Ref. 4. As Fig. (5.5) shows, we find less reduction in the height of the main peak for the same amount of relaxation as they considered ($\gamma_T/\gamma_1=0.1$). This is perhaps entirely due to the absence of diagonal relaxation in our model.

Finally, for ease of comparison with other calculations we give a table of parameter translations. The four basic parameters of all calculations are the asymmetry, universally denoted q, the autoionization linewidth, the detuning of the laser from the discrete-discrete transition frequency, $\Delta=\omega_{10}-\omega_L$, and some measure of laser field strength, usually called the Rabi frequency or generalized Rabi frequency. In four previous papers the expressions used for those parameters have the following

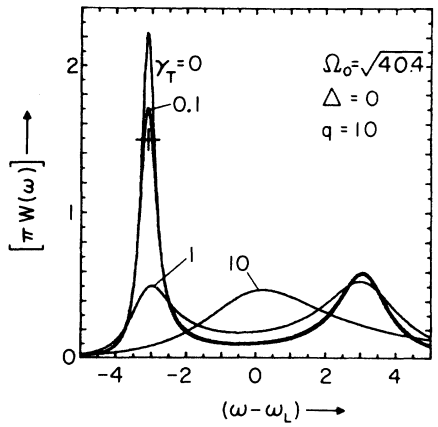

FIG. 13. Plots of the electron spectrum on resonance (no redistribution), showing the effects of γ_T. The cross marks the peak position achieved with *radiative* relaxation corresponding to $\gamma_T=0.1$. The unusual value of Ω_0 allows comparison with the curve labeled $\gamma=0.1$ in Fig. 3 of Agarwal, Haan, Burnett, and Cooper in Ref. 4 (see parameter translations given on next page).

translations into the present notation.

Lampropoulos and Zoller[3] (for $N \to 0$):

$$\delta = -\Delta = \omega_L - \omega_{10} ,$$

$$\kappa = \gamma_1 ,$$

$$\tilde{\Omega} = q\Omega_0/2(1+q^2)^{1/2} .$$

Rzążewski and Eberly[2]:

$$\Delta = \Delta ,$$

$$\gamma_0 = \gamma_1 ,$$

$$\Omega_0 = \Omega_0 .$$

Agarwal, Haan, Burnett, and Cooper[4]:

$$\alpha = -\Delta/\gamma_1 ,$$

$$\Gamma = 2\gamma_1 ,$$

γ = ratio of radiative linewidth to autoionization linewidth, comparable to our γ_T/γ_1

$$\Omega = w_q/\gamma_1 = \Omega_0^2/4(1+q^2)\gamma_1^2 .$$

Coleman and Knight[7]:

$$D = \Delta ,$$

$$\pi |\bar{V}_{\epsilon k}|^2 = \gamma_1 ,$$

$$\pi |\bar{V}_{\epsilon j}|^2 = w_q = \Omega_0^2/4(1+q^2)\gamma_1 .$$

VI. SUMMARY

We have presented the results of a theoretical study of laser-induced autoionization. We have used the simplest atomic model of Fano, but have considered a more general model of the laser-atom interaction. Our results are valid for strong as well as weak fields. They also take into account the existence of weak elastic collisions or a finite laser bandwidth, through a statistical treatment of the relative phase between the atomic dipole and the laser field.

In this paper we have confined our attention to the long-time photoelectron spectrum. The method we have used allows us to find the exact solutions of coupled stochastic integro-differential equations for Heisenberg operators (or density-matrix elements), not Schrodinger state amplitudes. It is also useful for obtaining finite-time expressions for atomic level populations, inversions, and dipole moments (also correlation functions). These further results will be published separately, although some aspects of them are already apparent in the electron spectrum (Rabi frequency, decay rate, asymptotic level populations, etc.).

We have shown that the spectrum, given in Eq. (5.6), is a surprisingly simple product of two Lorentzian functions (with Fano's interference preserved). We have found the positions and widths of the two spectral peaks in terms of a complex level shift L_q, given in closed form in (5.13) for arbitrary field strength. By comparison with other recent work on extensions of the Fano model to strong fields our results show the effect of an important type of line broadening, arising from off-diagonal (transverse) relaxation. The effects of transverse broadening are different from those of lifetime broadening. They include spectral redistribution, and our electron spectra are related in that respect to earlier results on transverse-broadened resonance fluorescence and Raman-scattered photon spectra. For arbitrary field strengths our electron spectrum contains the exact ac Stark shifts of the model, and cannot be written as a simple convolution of atomic and radiative line shapes.

Independent of the field strength of the inducing laser, it is clear that the Coulomb interaction in our (Fano's) model acts as a probe of the two-photon coupling between the original continuum states $|\omega\rangle$ and the excited discrete state $|1\rangle$. In that light, the present model has a wide range of analogs among three-level systems. However, three-level systems which incorporate a continuum have not been thoroughly studied yet. Our results indicate that the role of the asymmetry parameter q is more important than previously shown. For example, the new linewidth parameter w_q, defined in (5.10), is associated with field strengths that are not necessarily large but have still not been explored.

The confluence of coherences pointed out in RE is another element of the results given here. We have shown that the confluence is still present even under the influence of phase diffusion, and have explained why it is not disrupted by the relaxation processes in our model. The confluence shows that quantum interferences, such as give rise to Fano's zero in the electron excitation cross section, have more flexibility than a perturbative theory allows for them. This is apparent in Figs. 10 and 12(d) where near-confluent scattering is highly inelastic (energy nonconserving in finite-order perturbation theory).

Other authors have recently used similar atomic and radiation models to describe aspects of laser-induced autoionization. None have yet included the effects of purely off-diagonal relaxation as we have, although there have recently appeared calculations that do include radiative relaxation. Apart from the inclusion of relaxation or not, there is little difference among the models used. Some authors employ dressed atom-photon states in calculations with quantized fields, but no consequences of such field

quantization have been pointed out. Similarly, some authors include processes such as higher transitions within the continuum, or take somewhat more careful account of the ionization edge than we have done. These are potentially important in the right circumstances,[24] certainly, but probably no more important than effects almost universally ignored, such as optical pumping within additional (lower) bound states or the finite duration of the laser pulse.

At the present it appears that the neglect of small obvious effects, or the near similarity of models, is appropriate in theoretical studies of laser-induced autoionization. The results are expected to be widely applicable, and not only to atomic systems. These calculations thus serve the purpose of identifying the parameters that retain their significance from one atomic species to another and from one to another configuration of atomic energy levels. They give the overall shapes of spectral curves, rather than specific numerical predictions.

ACKNOWLEDGMENTS

We thank D. Agassi for a careful independent solution of our integro-differential equations and for helpful discussions. The final form of the spectrum in Eq. (5.6) and the calculation of peak heights is due to Q. Lu. We are grateful to B. J. Herman for important assistance during the preparation of the manuscript. This research was supported in part by the U.S. Air Force Office of Scientific Research under Grant number AFOSR-81-0204-A.

APPENDIX: SOLUTION OF STOCHASTIC INTEGRO-DIFFERENTIAL EQS. (2.4)

There is a well-known result from the theory of multiplicative stochastic processes that applies to a stochastic differential equation such as

$$dQ/dt=[L_0+x(t)L_1]Q\ , \tag{A1}$$

where Q is a vector function of time and L_0 and L_1 are (possibly noncommuting) constant matrices. Here $x(t)$ is a Gaussian stochastic process satisfying the white-noise condition

$$\langle\langle x(t_1)x(t_2)\rangle\rangle=2\beta\delta(t_1-t_2)\ , \tag{A2}$$

where double brackets indicate an average over the ensemble of realizations of the process $x(t)$. This result is that $\langle\langle Q\rangle\rangle$ exactly satisfies the *nonstochastic* equation

$$d\langle\langle Q\rangle\rangle/dt=(L_0+\beta L_1^2)\langle\langle Q\rangle\rangle\ . \tag{A3}$$

Such an equation, having constant coefficients, is appropriately studied in the Laplace transform domain.

These facts are applicable to the quantum-mechanical expectation values of Eqs. (3.10a)–(3.10c), given Eq. (3.1). The initial conditions appropriate to a discussion of ionization are

$$\hat{P}_0\Big|_{t=0}=1\ , \tag{A4a}$$

$$\hat{B}_\omega\Big|_{t=0}=\hat{C}_{\omega\omega'}\Big|_{t=0}=0\ . \tag{A4b}$$

We will denote with a tilde the Laplace transform of the exact quantum-mechanical and stochastic average of one of the variables. For example,

$$\tilde{P}_0(z)\equiv\int_0^\infty dt\, e^{-zt}\langle\langle\hat{P}_0(t)\rangle\rangle\ , \tag{A5}$$

etc. Then, in place of Eq. (3.10), we have

$$z\tilde{P}_0-1=-i\int d\omega\,\Omega_\omega\tilde{B}_\omega+\text{c.c}\ , \tag{A6a}$$

$$[z+i(\omega-\omega_L)+\gamma_L]\tilde{B}_\omega=-i\Omega_\omega^*\tilde{P}_0+i\int d\omega'\Omega_{\omega'}^*\tilde{C}_{\omega'\omega}\ , \tag{A6b}$$

$$[z-i(\omega-\omega')]\tilde{C}_{\omega\omega'}=i\Omega_\omega\tilde{B}_{\omega'}-i\Omega_{\omega'}^*\tilde{B}_\omega^*\ . \tag{A6c}$$

Equation (A6c) is used to eliminate $\tilde{C}_{\omega\omega'}$, and Eqs. (A6a) and (A6b) are simply written using

$$\tilde{D}_\omega\equiv\Omega_\omega\tilde{B}_\omega\ . \tag{A7}$$

We find

$$z\tilde{P}_0=1-i\int d\omega(\tilde{D}_\omega-\tilde{D}_\omega^*)\ , \tag{A8}$$

$$\tilde{D}_\omega=\frac{|\Omega_\omega|^2}{\mathscr{H}(z,\omega)}\int d\omega'\frac{\tilde{D}_{\omega'}^*}{z+i(\omega-\omega')}-i\frac{|\Omega_\omega|^2}{\mathscr{H}(z,\omega)}\tilde{P}_0\ , \tag{A9}$$

where

$$\mathscr{H}(z,\omega)=z+\gamma_L+i(\omega-\omega_L)+\int d\omega'\frac{|\Omega_{\omega'}|^2}{z+i(\omega-\omega')}\ . \tag{A10}$$

By combining (A9) with its complex conjugate (note that complex conjugation does not affect the Laplace variable z), $\tilde{D}_\omega^*$ can be eliminated, and we find

$$\tilde{D}_\omega=\frac{|\Omega_\omega|^2}{\mathscr{H}(z,\omega)}\int d\omega''\tilde{D}_{\omega''}\int d\omega'\frac{1}{z+i(\omega-\omega')}\frac{|\Omega_\omega|^2}{\mathscr{H}^*(z,\omega)}\frac{1}{z-i(\omega'-\omega'')}+i\frac{|\Omega_\omega|^2}{\mathscr{H}(z,\omega)}\left[\int d\omega'\frac{1}{z+i(\omega-\omega')}\frac{|\Omega_\omega|^2}{\mathscr{H}^*(z,\omega)}-1\right]\tilde{P}_0\ . \tag{A11}$$

Equation (A11) is an inhomogeneous Fredholm integral equation, with kernel

$$K(\omega,\omega'')=\int d\omega' \frac{1}{z+i(\omega-\omega')} \frac{|\Omega_\omega|^2}{\mathscr{H}^*(z,\omega')} \times \frac{1}{z-i(\omega'-\omega'')} . \quad \text{(A12)}$$

Therefore (A11) can be solved analytically if a spectral decomposition of K is possible. The simplest examples occur when $|\Omega_\omega|^2$ is either Lorentzian in form (Sec. IV) or a sum of Lorentzians (Sec. V). For example, if we let $q\to\infty$ in Ω_ω we get

$$|\Omega_\omega|^2=\tfrac{1}{4}\Omega_0^2 \frac{\gamma_1/\pi}{(\omega-\omega_{10})^2+\gamma_1^2} , \quad \text{(A13)}$$

in which case K is factorable:

$$K(\omega,\omega')=A_1(\omega)A_2(\omega') . \quad \text{(A14)}$$

The remainder of the solution for $q\to\infty$ is straightforwardly tedious, and leads to two principal results. First, the time-dependent probability to remain in the ground state is found to be

$$P_0(t)=\int \frac{dz}{2\pi i} U^{-1}(z)e^{zt} , \quad \text{(A15)}$$

where

$$U(z)=z+\frac{\frac{1}{2}\Omega_0^2(z+2\gamma_1)(z+\gamma_1+\gamma_T)}{(z+2\gamma_1)[(z+\gamma_1+\gamma_T)^2+\Delta^2]+\frac{1}{2}\Omega_0^2(z+\gamma_1+\gamma_T)} . \quad \text{(A16)}$$

Here Δ denotes the detuning of the autoionization resonance from the laser:

$$\Delta\equiv\omega_{10}-\omega_L . \quad \text{(A17)}$$

Second, the spectral distribution of excited electrons can be determined from $C_{\omega\omega}(t)$. This is most easily obtained in the steady state (steady state corresponds, here, to complete ionization) at $t=\infty$ when only the pole at $z=0$ in the Laplace domain contributes. From (A6c) one obtains

$$\tilde{C}_{\omega\omega}(z)=(i/z)[\tilde{D}_\omega(z)-\tilde{D}^*_\omega(z)] . \quad \text{(A18)}$$

Thus the spectrum $W(\omega)$ is given by

$$W(\omega)=i[\tilde{D}_\omega(0)-\tilde{D}^*_\omega(0)] . \quad \text{(A19)}$$

In Sec. V we indicate the generalizations necessary if q is finite. The explicit form of W is explored in Secs. IV and V.

*Permanent address: Institute of Theoretical Physics, Polish Academy of Sciences, 02-668 Warsaw, Poland.

[1]U. Fano, Phys. Rev. 124, 1866 (1961).

[2]K. Rzążewski and J. H. Eberly, Phys. Rev. Lett. 47, 408 (1981).

[3]P. Lambropoulos, Appl. Opt. 19, 3926 (1980); see also P. Lambropoulos and P. Zoller, Phys. Rev. A 24, 379 (1981); and Z. Bialynicka-Birula (unpublished).

[4]G. S. Agarwal, S. L. Haan, K. Burnett, and J. Cooper, Phys. Rev. Lett. 48, 1164 (1982); S. L. Haan and G. S. Agarwal, in *Proceedings of the Sixth International Conference on Spectral Line Shapes,* edtied by K. Burnett (de Gruyter, Berlin, 1982); see also L. Armstrong, Jr., C. E. Theodosiou, and M. J. Wall, Phys. Rev. A 18, 2538 (1978).

[5]L. Armstrong, Jr., B. L. Beers, and S. Feneuille, Phys. Rev. A 12, 1903 (1975); M. Crance and L. Armstrong, J. Phys. B (in press).

[6]Yu. I. Heller and A. K. Popov, Opt. Comm. 18, 449 (1976); Yu. I. Heller, V. F. Lukinykh, A. K. Popov, and V. V. Slabko, Phys. Lett. 82A, 4 (1981); and other references therein.

[7]P. E. Coleman and P. L. Knight, J. Phys. B 15, L235 (1982), and corrigendum, *ibid.* 15, 1957 (1982); see also P. M. Radmore and P. L. Knight, *ibid.* 15, 561 (1982).

[8]A. I. Andryushin, A. E. Kazakov, and M. V. Fedorov, Zh. Eksp. Teor. Fiz. 82, 91 (1982) [Sov. Phys.—JETP 55, 53 (1982)].

[9]See, for example, A. Omont, E. W. Smith, and J. Cooper, Astrophys. J. 175, 185 (1972); B. R. Mollow, Phys. Rev. A 15, 1023 (1977); J. L. Carlsten, A. Szöke, and M. G. Raymer, *ibid.* 15, 1029 (1977); K. Burnett, J. Cooper, P. D. Kleiber, and A. Ben Reuven, *ibid.* 25, 1345 (1982). In the context of autoionization, see the comment by J. H. Eberly, K. Rzążewski, and D. Agassi, Phys. Rev. Lett. 49, 693 (1982).

[10]For example, see L. Allen and J. H. Eberly, *Optical Resonance and Two-Level Atoms* (Wiley, New York, 1975), for an introduction to two-level concepts such as Rabi frequency and rotating-wave approximation.

[11]S. H. Autler and C. H. Townes, Phys. Rev. 100, 703 (1955).

[12]Examples of applications of the Wiener-Levy phase diffusion model in quantum optics can be found in P. Zoller, J. Phys. B 10, L321 (1977); 11, 805 (1978); G. S. Agarwal, Phys. Rev. A 18, 1490 (1978); K. Wódkiewicz, *ibid.* 19, 1686 (1979).

[13]An examination of various discrete-continuum transition effects, on general semiqualitative grounds, is presented by C. Cohen-Tannoudji, B. Diu, and F. Laloe in *Quantum Mechanics* (Wiley, New York, 1977), pp. 1343–1350. The model represented in (4.1) has also

been used to derive equations for two-photon ionization. See J. L. F. De Meijere and J. H. Eberly, Phys. Rev. A 17, 1416 (1978).

[14]It may become apparent that, on very general grounds, the one-Lorentzian autoionized electron spectrum has close connections with the emitted-photon spectrum computed for strongly driven discrete-discrete transitions by B. R. Mollow, Phys. Rev. A 5, 1522 (1972); 8, 1949 (1973); see also P. Zoller, J. Phys. B 11, 805 (1978); J. Cooper and A. Szöke, Phys. Rev. A 23, 378 (1981).

[15]P. E. Coleman and P. L. Knight, Phys. Lett. 81A, 383 (1981); see also P. E. Coleman and P. L. Knight, J. Phys. B 14, 2139 (1981), and earlier work quoted therein.

[16]See, for example, P. L. Knight, J. Phys. B 12, 3297 (1979) and *Laser Physics,* edited by D. F. Walls and J. Harvey (Academic, Sydney, 1980), p. 92.

[17]P. L. Knight, W. A. Molander, and C. R. Stroud, Jr., Phys. Rev. A 17, 1547 (1978); see also M. G. Raymer and J. Cooper, *ibid.* 20, 2238 (1979).

[18]M. G. Raymer and J. L. Carlsten, Phys. Rev. Lett. 39, 1326 (1977); M. G. Raymer, Ph.D. thesis, University of Colorado, 1979 (unpublished); M. G. Raymer, J. L. Carlsten, and G. Pichler, J. Phys. B 12, L119 (1979).

[19]D. Agassi, K. Rzążewski, and J. H. Eberly (unpublished).

[20]S. Feneuille, S. Liberman, J. Pinard, and A. Taleb, Phys. Rev. Lett. 42, 1404 (1979); see also Yu. I. Heller and A. K. Popov, Opt. Commun. 18, 449 (1976); Yu. I. Heller, V. F. Lukinykh, A. K. Popov, and V. V. Slabko, Phys. Lett. 82A, 4 (1981).

[21]B. L. Beers and L. Armstrong, Jr., Phys. Rev. A 12, 2447 (1975).

[22]J. H. Eberly, D. Agassi, and K. Rzążewski (unpublished).

[23]That is, the indifference of Fano interference to a finite γ_T is due entirely to the "V" character of the two-photon transition. A two-photon cascade-type transition would be quite sensitive to the size of γ_T.

[24]For a treatment of a discrete-continuum transition in which the ionization edge plays an essential role, under the influence of a strong laser field, see K. Rzażewski, M. Lewenstein, and J. H. Eberly, J. Phys. B 15, L661 (1982).